Journal of Materials Chemistry C

RSC Publishing

PAPER

View Article Online
View Journal | View Issue

Cite this: J. Mater. Chem. C, 2013, 1, 7731

Practical access to bandgap-like N-doped carbon dots with dual emission unzipped from PAN@PMMA core–shell nanoparticles†

Youfu Wang, Luhua Dong, Rulin Xiong and Aiguo Hu*

Received 21st May 2013
Accepted 29th August 2013

DOI: 10.1039/c3tc30949e

www.rsc.org/MaterialsC

As emergent nanolights for bioimaging, catalysis, sensors, and photoelectronics, carbon dots (C-dots) have attracted much research attention. However, the practical and scalable preparation of C-dots has been less explored, even after various top-down and bottom-up approaches being reported recently. To this end, we discover a new approach to prepare C-dots by simply unzipping core–shell polymeric nanoparticles, prepared by a microemulsion polymerization. Uniformly distributed N-doped C-dots are prepared by the pyrolysis of PAN@PMMA core–shell nanoparticles at different temperatures, followed by dialysis. TEM analysis shows that many of the C-dots of 2–3 nm size are unzipped from each polymeric particle. All the purified C-dots show a bandgap-like photoluminescence (PL) behaviour, with dual emission and a stable PL between pH 5–12.

Introduction

Photoluminescent materials are getting more and more attention because of their wide applications in everyday life and specialized fields such as bioimaging, catalysis, sensors, and photoelectronics. During the past several decades, considerable efforts have been made to expand the library of fluorescent materials, which includes semiconductor quantum dots,[1] lanthanide chelates,[2] core–shell silica nanoparticles[3] and carbon dots (C-dots). By virtue of their biocompatibility, low toxicity, and ease of preparation, C-dots are environmentally benign alternatives to quantum dots comprised of heavy metals.[4–6]

Since their serendipitous discovery in 2004[7] when researchers tried to purify carbon nanotubes by gel electrophoresis, C-dots have been magnificently transformed into nanolights in a variety of applications.[5,6,8] The preparation of C-dots varies in many different strategies. Using the "top-down" approach, pristine C-dots are broken off from mass carbon materials through arc-discharge, laser-ablation[8,9] and electrochemical soaking,[10–12] followed by chemical treatment. Using the "bottom-up" approach, C-dots are formed through the agglomeration of the carbon content generated from decomposition,[13] microwave[14] or hydrothermal[15] treatment, and pyrolysis[16] of small organic molecules. Using the "bijective" approach, each C-dot is generated from one single polymeric nanoparticle following the "bijective pairing" rule.[17]

N-doping is a widely used approach to tune the PL behaviour of photoluminescent materials.[18–20] Qu *et al.* developed an effective electrochemical strategy to generate N-doped graphene quantum dots (GQDs).[19] The N-doped GQDs showed distinctive optoelectronic, electrocatalytic, and luminescent features from their N-free counterparts. Giannelis *et al.*[18] prepared N-doped C-dots by the pyrolytic decomposition of citric acid and ethanolamine (1 : 3 molar ratio) at different temperatures and found that the N-doped C-dots showed a dual emission behaviour. The authors also elaborated the photoluminescent mechanism of the C-dots, which arises from the excitation state of the core domains and the surface chemistry.

Even after various top-down and bottom-up approaches being reported recently, the practical and scalable preparation of C-dots has been less explored. Herein, we apply a new approach to prepare photoluminescent N-doped C-dots by unzipping core–shell polymeric nanoparticles (PAN@PMMA) prepared by a microemulsion polymerization on a large scale. In this approach, many C-dots are generated from each polymeric nanoparticle. The PAN core domains are broken into several carbon-rich domains inlaying the PMMA shell domains, which prevent the aggregation of these C-dots. Uniform C-dots are prepared by the pyrolysis of the polymeric nanoparticles at different temperatures, followed by purification through dialysis. All the purified C-dots show a bandgap-like PL behaviour with a fixed dual emission and show pyrolysis temperature-dependent and λ_{ex}-independent emissions, which is different from the trends typically found in the C-dots reported previously. Almost no change in the emission wavelength and PL

Shanghai Key Laboratory of Advanced Polymeric Materials, School of Materials Science and Engineering, East China University of Science and Technology, Shanghai, 200237, China. E-mail: hagmhsn@ecust.edu.cn; Fax: +86-21-64253037; Tel: +86-21-64253037

† Electronic supplementary information (ESI) available: Detailed experimental procedures and characterization by HRTEM, Raman, UV-vis and PL spectra, XPS, and TGA. See DOI: 10.1039/c3tc30949e

intensity is observed between pH 5–12, which is essential for physiological imaging applications.

Experimental section

Materials

All of the reactions and manipulations were carried out under nitrogen with the use of a standard inert atmosphere and Schlenk techniques. Methyl methacrylate (MMA) was passed through an alkaline Al_2O_3 column to remove the inhibitor before use. Acrylonitrile (AN) was flash distilled before use. All the other reagents were commercially available and used as received. Deionized water was used in all the experiments.

Characterizations

Transmission electron microscopy (TEM) images were taken on a JEOL JEM-1400 microscope (JEOL, Japan) at an acceleration voltage of 100 kV. The as-synthesized PAN@PMMA samples were first diluted with deionized water and incubated on a 400-mesh copper grid at room temperature. The grid was stained with 2% (w/v) phosphonium tungsten acid for 20 seconds and then delivered into the TEM chamber for imaging. The size and size distribution of the polymeric nanoparticles were determined by dynamic light scattering (DLS) at 25 °C using a Delsa TM Nano particle size analyser (Beckman Coulter, US) and were reported as the number average diameter. High-resolution TEM (HRTEM) images were obtained on a JEOL JEM-2100 microscope (JEOL, Japan) at an acceleration voltage of 200 kV. Thermogravimetric analysis (TGA) was carried out on a SPA409PC Thermal Analyser. The samples were heated at a constant rate of 5 °C min^{-1} from room temperature to 600 °C under an air flow. The photoluminescence (PL) and UV-vis spectra of the C-dots were taken at room temperature in aqueous solutions of different pH values. The PL spectra were collected on a Fluorolog-3-P UV-VIS-NIR fluorescence spectrophotometer (Jobin Yvon, France) and the UV-vis spectra were obtained using a UNICO UV-21-2 PCS spectrometer. XPS experiments were carried out on an ESCALAB 250Xi system (Thermo Fisher) with Al Kα radiation ($h\nu = 1486.6$ eV). Raman measurements were performed on an inVia-reflex Raman spectrometer (Renishaw, 785 nm).

Preparation of PAN@PMMA core–shell nanoparticles

The PAN@PMMA core–shell nanoparticles were prepared through a differential microemulsion polymerization according to Rempel's method.[22,23] The polymerization was carried out under a nitrogen atmosphere. Typically, sodium dodecyl benzene sulfonate (SDBS, 1.26 g) was first dissolved in deionized water (84 mL) at room temperature to form a homogeneous solution in a three-necked flask. After the subsequent addition of benzoyl peroxide (BPO, 0.086 g) powder into the solution, the resulting mixture was subjected to magnetic stirring to form a homogeneous solution and heated up to 70 °C under nitrogen, and maintained for 1.5 h. Then, AN (5 mL) was added in a differential manner at a given rate of 0.15 ± 0.02 mL min^{-1} *via* a dropping funnel. After completion of the AN addition, the reaction system was kept at 70 °C for 0.5 h. The temperature was further increased to 83 °C, and then MMA (8 mL) was added in a similar manner. After the addition of the MMA, the reaction system was aged for an additional hour. The polymerization was finally stopped by immersing the flask in an ice/water bath.

Preparation of photoluminescent C-dots

Carbonization. The as-synthesized aqueous polymeric nanoparticles (1 mL) were subjected to a quartz boat and heated under a continuous air flow in a tube furnace at a heating rate of 2 °C min^{-1} from room temperature to 270 °C, and maintained for 2 h to cross-link the PAN part (core domains) of the nanoparticles. The temperatures was then increased to 350 °C, 400 °C and 450 °C at 5 °C min^{-1}, and maintained for 1 h to decompose the PMMA part (shell domains) of the nanoparticles as well as carbonize the final C-dots.

Bare C-dots. The raw carbon materials were added to 5 M HNO_3 (6 mL), and the mixture was refluxed at 120 °C for 12 h. After neutralization with sodium bicarbonate, the C-dots were desalted by dialysis (MWCO 1000) against deionized water for 2 days. Then, the desalted C-dots were purified by dialysis (MWCO 7000) to get uniform C-dots, and referenced as CD-350, CD-400 and CD-450 depending on the pyrolysis temperatures, respectively.

Surface modification. 0.2 g diamine-terminated PEG_{2000N} was added to the C-dots solution and the mixture was heated to 120 °C for 3 days for surface modification, and referenced as CD-350-PEG, CD-400-PEG and CD-450-PEG, respectively.

Quantum yield (QY) measurements

Quinine sulphate in 0.1 M H_2SO_4 (QY = 0.54 at 350 nm) was chosen as a standard.[20] The quantum yield of the C-dots in water was calculated according to the following equation:

$$\phi = \phi_r \times \frac{A_r}{I_r} \times \frac{I}{A} \times \frac{n^2}{n_r{}^2}$$

where ϕ is the quantum yield, I is the measured integrated emission intensity, n is the refractive index (1.33 for water), and A is the optical density. The subscript "r" refers to the reference fluorophore of known quantum yield. In order to minimize reabsorption effects, the absorbencies in the 10 mm fluorescence cuvette were kept under 0.1 at the excitation wavelength of 340 nm.

Results and discussion

To get uniformly distributed C-dots, uniformly distributed carbon-yielding domains are necessary, which can be stabilized and transformed to C-dots during the pyrolysis. Space domains are also needed to prevent the aggregation of C-dots-generating domains during the pyrolysis, and they should be decomposed at a suitable temperature. Core–shell nanostructured polymeric particles (Fig. 1A) are the choice satisfying both of these requirements.[21] Uniform PAN@PMMA core–shell nanoparticles were prepared through a differential microemulsion polymerization according to Rample's method.[22,23] It is essential to add

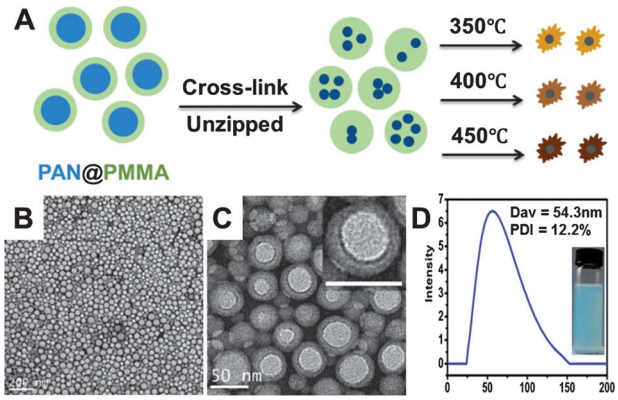

Fig. 1 (A) Schematic illustration of the preparation of C-dots unzipped from PAN@PMMA core–shell nanoparticles. Many N-doped carbon dots were unzipped from one polymeric nanoparticle and show different PL behaviours at different pyrolysis temperatures. (B–C) TEM images of the PAN@PMMA core–shell nanoparticles. Scale bars are 200 nm (B) and 50 nm (C), respectively. (D) DLS curve of the PAN@PMMA core–shell nanoparticles; the inset shows a photograph of a PAN@PMMA microemulsion.

monomers in a very slow and controlled manner. The TEM images of the PAN@PMMA nanoparticles are shown in Fig. 1B and C. Core–shell structured spherical particles of 50 nm size can be clearly seen in the images, with the shell domain selectively stained by the tungsten agent. The particle size and size distribution were also obtained with dynamic light scattering (DLS) and are shown in Fig. 1D, which are consistent with the results obtained with TEM.

The necessary stabilization of the carbon-yielding domains was achieved by thermal treatment (heating to 270 °C in the presence of air), a process well-known in the fabrication of carbon fibres,[24] which causes the PAN precursor to form a cyclic, ladder, and eventually a crosslinked species. The nitrogen atoms in the PAN domain are essential to tune the PL properties of the final C-dots.[19,25] The TEM images of the carbonaceous materials after pyrolysis at 270 °C in air (Fig. 2) show that the core domains were unzipped into many parts, which may generated from the asymmetrical shrinkage of the PAN precursor during crosslinking. Uniform carbon-rich domains of size about 2–3 nm were formed and dispersed in the amorphous carbonaceous matrix at this stage. The amorphous carbonaceous materials may originate from the aggregation of the shell domains PMMA, which was essential to prevent the interparticle crosslinking and agglomeration. Thermogravimetric analysis (TGA) showed that the shell domain completely decomposed after the sample was heated at 350 °C in air (Fig. S2†). Therefore, high temperature thermal treatments at 350 °C, 400 °C and 450 °C were conducted to remove the PMMA shell domains and further carbonize the PAN core domains. After surface activation in HNO_3 followed by desalination and dialysis against deionized water, homogeneous solutions with colourless to light brown colour were obtained (Fig. S1A†), referenced as CD-350, CD-400 and CD-450 depending on the pyrolysis temperatures, respectively. The HRTEM image and size distribution of CD-450 are shown in Fig. 2 (HRTEM images of CD-350 and CD-400 are shown in Fig. S3†). The diameters of these C-dots centres at 2.1 nm, and the pyrolysis temperature showed a slight influence on the size or size distribution of the C-dots.

UV-vis and PL spectra of CD-450 are shown in Fig. 3a, the spectra of CD-350 and CD-400 are shown in Fig. S4.† All these C-dots exhibited a dual emission at λ_{em} of around 410 and 450 nm. The wavelengths of these emissions did not change when the C-dots were under irradiation of λ_{ex} between 310 and 360 nm. This λ_{ex}-independent PL behaviour was different from the trends typically found in the C-dots reported in previous work. The uncommon PL properties of the C-dots were similar to the bandgap-like PL of molecular dyes like amide groups, which consists of chromophores undergoing direct singlet-to-triplet transitions and showing a strong PL emission at around 455 nm.[26] The emission at 450 nm may originate from the bandgap-like transition of the amide groups (or imine groups) in the C-dots, and the emission at 410 nm may originate from the amorphous carbonaceous core. Fig. 3b shows the normalized PL spectra of the three kinds of C-dots under excitation at 310 nm. Interestingly, the shape of the PL spectrum of CD-400 was different from those of CD-350 and CD-450. A spectrum deconvolution showed that the intensity ratio of the two emission peaks (I_{450}/I_{410}) of CD-400 is higher than that of CD-350 and CD-450, indicating a greater contribution of the amide

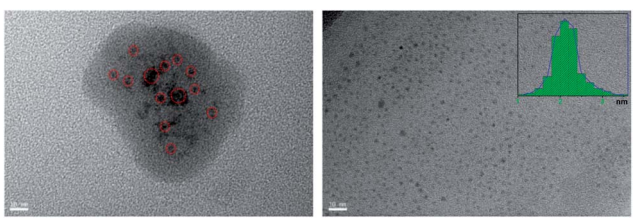

Fig. 2 HRTEM images of carbonaceous materials (left) after pyrolysis of the PAN@PMMA at 270 °C in air and CD-450 (right) with the inset showing the size distribution. Scale bar: 10 nm.

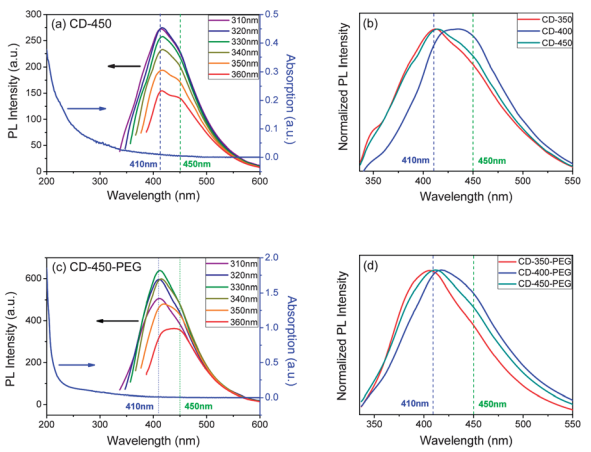

Fig. 3 (a) UV-vis and PL spectra of CD-450, (b) normalized PL spectra of C-dots pyrolyzed at different temperatures under $\lambda_{ex} = 310$ nm irradiation. (c) UV-vis and PL spectra of CD-450-PEG, (d) normalized PL spectra of C-dots pyrolyzed at different temperatures under $\lambda_{ex} = 310$ nm irradiation.

groups (or imine groups) to the PL in these C-dots. The higher population of amide groups (or imine groups) in CD-400 was also evidenced by the XPS analysis. Fig. 4 shows the XPS spectra of three kinds of C-dots. The C 1s peaks consist of sp^2 C=C at the binding energy of 284.9 eV, and other sub-bands of C–N (amide, 285.6 eV), C–O (hydroxyl and epoxy, 286.1 eV), C=N (imine and amide, 287.0 eV), C=O (carbonyl, 288.7 eV) and O–C=O (carboxyl, 289.9 eV) groups. The content of the amide groups (or imine groups) in CD-400 is higher than that in CD-350 and CD-450. Raman spectroscopy (Fig. S6†) further confirms the higher content of the amide groups in CD-400. The G band at 1590 cm^{-1} is related to the in-plane E_{2g} vibration mode of graphite sp^2-bonded carbon atoms, and the D band at 1350 cm^{-1} is attributed to graphitic carbon, with structural defects. The intensity ratio of the G and D bands (I_G/I_D) in CD-400 is much lower than that in other C-dots, indicative of the presence of higher contents of amide groups, which are structural defects in graphitic carbon of C-dots. When the pyrolysis temperature was increased from 350 °C to 400 °C, the carbon and nitrogen atoms on the surface of the C-dots was oxidized by the oxygen in air, generating a high content of amide groups. Further increasing the pyrolysis temperature resulted in slowly burning off these surface bounded amide groups, restoring the ratio of graphitic carbon and amide groups. Therefore, CD-350 and CD-450 showed similar PL behaviour, while CD-400 showed a stronger emission at a longer wavelength (450 nm).

The surface modification of C-dots is a well acknowledged procedure to improve the dispersibility of C-dots in solvents, which may suppress the aggregate-induced energy–charge transfer process. As a result, the quantum yield (QY) of C-dots can be greatly boosted. All the C-dots were therefore treated with a diamine-terminated polyethylene glycol (PEG_{2000N}) and denoted as CD-350-PEG, CD-400-PEG and CD-450-PEG, respectively. UV-vis and PL spectra of CD-450-PEG are shown in Fig. 3c,

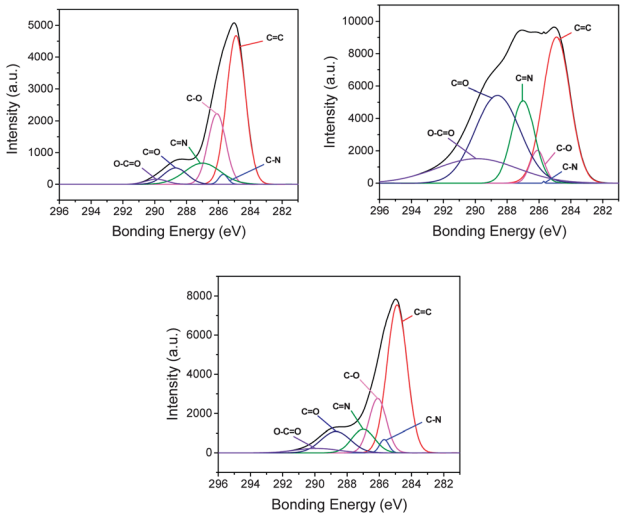

Fig. 4 The C 1s peaks in the XPS spectra of CD-350 (top left), CD-400 (top right) and CD-450 (bottom). The curve was fitted considering the following contributions: C=C, C–N (amide), C–O (hydroxyl and epoxy), C=N (imine and amide), C=O (carbonyl) and O–C=O (carboxyl) groups.

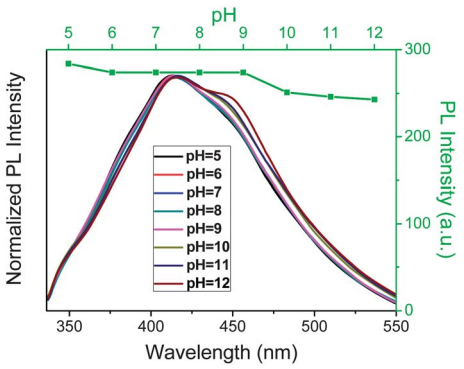

Fig. 5 Normalized PL spectra of CD-450 in diverse pH solutions under 310 nm irradiating. The green dot dash lines show the maximum PL intensity during pH 5–12.

the spectra of CD-350-PEG and CD-400-PEG are shown in Fig. S7.† All these PEG-modified C-dots showed a fixed dual emission at 410 nm and 450 nm under an irradiation of λ_{ex} between 310 and 360 nm, similar to those of the bare C-dots. Interestingly, a significant increase in the QY from 7% to 24% was observed after the PEG-modification (photographs of the PEG modified C-dots are shown in Fig. S1B†).

All these C-dots exhibited a pH-independent PL behaviour; no clear change in the emission position or the PL intensity was observed during pH 5–12 (Fig. 5). This can be attributed to the coexistence of amide groups and carboxyl groups on the surface of the C-dots, rendering an unaffected surface chemistry in a wide range of pH. The stable PL emission of the C-dots is essential in biological imaging.

Conclusions

We have developed a practical and facile approach for the fabrication of photoluminescent C-dots through a well-controlled procedure; the pyrolysis of core–shell polymeric nanoparticles, followed by dialysis. TEM analysis showed many C-dots were unzipped from each polymeric nanoparticle. All these C-dots showed a bandgap-like PL behaviour with a fixed dual emission. The contents of the PL-active components could be varied by adjusting the pyrolysis temperatures. Surface modification with PEG did not show any influence on the PL energy of the carbon dots, but boosted the QYs. All the C-dots showed a pH-stable PL behaviour, which is important for fluorescent imaging under an physiological environment. As PAN@PMMA core–shell nanoparticles can be massively prepared by a microemulsion polymerization in industry, C-dots can thus be fabricated in a large scale through this process.

The authors gratefully acknowledge the financial support from National Natural Science Foundation of China (21274042, 20874026), the Shanghai Shuguang Project (07SG33) and the Shanghai Leading Academic Discipline Project (B502). A. H. thanks Prof. Lingyong Zhu for his valuable comments on this work.

Notes and references

1 L. Qu and X. Peng, *J. Am. Chem. Soc.*, 2002, **124**, 2049–2055.
2 M. Li and P. R. Selvin, *J. Am. Chem. Soc.*, 1995, **117**, 8132–8138.
3 A. Burns, H. Ow and U. Wiesner, *Chem. Soc. Rev.*, 2006, **35**, 1028–1042.
4 S.-T. Yang, L. Cao, P. G. Luo, F. Lu, X. Wang, H. Wang, M. J. Meziani, Y. Liu, G. Qi and Y.-P. Sun, *J. Am. Chem. Soc.*, 2009, **131**, 11308–11309.
5 S. N. Baker and G. A. Baker, *Angew. Chem., Int. Ed.*, 2010, **49**, 6726–6744.
6 J. H. Shen, Y. H. Zhu, X. L. Yang and C. Z. Li, *Chem. Commun.*, 2012, **48**, 3686–3699.
7 X. Xu, R. Ray, Y. Gu, H. J. Ploehn, L. Gearheart, K. Raker and W. A. Scrivens, *J. Am. Chem. Soc.*, 2004, **126**, 12736–12737.
8 Y.-P. Sun, B. Zhou, Y. Lin, W. Wang, K. A. S. Fernando, P. Pathak, M. J. Meziani, B. A. Harruff, X. Wang, H. Wang, P. G. Luo, H. Yang, M. E. Kose, B. Chen, L. M. Veca and S.-Y. Xie, *J. Am. Chem. Soc.*, 2006, **128**, 7756–7757.
9 S.-L. Hu, K.-Y. Niu, J. Sun, J. Yang, N.-Q. Zhao and X.-W. Du, *J. Mater. Chem.*, 2009, **19**, 484–488.
10 Q.-L. Zhao, Z.-L. Zhang, B.-H. Huang, J. Peng, M. Zhang and D.-W. Pang, *Chem. Commun.*, 2008, 5116.
11 J. Zhou, C. Booker, R. Li, X. Zhou, T.-K. Sham, X. Sun and Z. Ding, *J. Am. Chem. Soc.*, 2007, **129**, 744–745.
12 L. Bao, Z. L. Zhang, Z. Q. Tian, L. Zhang, C. Liu, Y. Lin, B. P. Qi and D. W. Pang, *Adv. Mater.*, 2011, **23**, 5801–5806.
13 A. B. Bourlinos, A. Stassinopoulos, D. Anglos, R. Zboril, V. Georgakilas and E. P. Giannelis, *Chem. Mater.*, 2008, **20**, 4539–4541.
14 X. Wang, K. Qu, B. Xu, J. Ren and X. Qu, *J. Mater. Chem.*, 2011, **21**, 2445–2450.
15 Y. H. Yang, J. H. Cui, M. T. Zheng, C. F. Hu, S. Z. Tan, Y. Xiao, Q. Yang and Y. L. Liu, *Chem. Commun.*, 2012, **48**, 380–382.
16 R. L. Liu, D. Q. Wu, S. H. Liu, K. Koynov, W. Knoll and Q. Li, *Angew. Chem., Int. Ed.*, 2009, **48**, 4598–4601.
17 B. Zhu, S. Sun, Y. Wang, S. Deng, G. Qian, M. Wang and A. Hu, *J. Mater. Chem. C*, 2013, **1**, 580–586.
18 M. J. Krysmann, A. Kelarakis, P. Dallas and E. P. Giannelis, *J. Am. Chem. Soc.*, 2012, **134**, 747–750.
19 Y. Li, Y. Zhao, H. Cheng, Y. Hu, G. Shi, L. Dai and L. Qu, *J. Am. Chem. Soc.*, 2011, **134**, 15–18.
20 J. R. Lakowicz, in *Principles of Fluorescence Spectroscopy*, Kluwer Academic/Plenum Publishers, New York, 1999.
21 A.-H. Lu, T. Sun, W.-C. Li, Q. Sun, F. Han, D.-H. Liu and Y. Guo, *Angew. Chem., Int. Ed.*, 2011, **50**, 11765–11768.
22 H. Wang, Q. Pan and G. L. Rempel, *Eur. Polym. J.*, 2011, **47**, 973–980.
23 H. Wang, Q. Pan, M. Hammond and G. L. Rempel, *J. Polym. Sci., Part A: Polym. Chem.*, 2012, **50**, 736–749.
24 P. Bajaj and A. Roopanwal, *J. Macromol. Sci., Part C*, 1997, **37**, 97–147.
25 S. Liu, L. Wang, J. Tian, J. Zhai, Y. Luo, W. Lu and X. Sun, *RSC Adv.*, 2011, **1**, 951–953.
26 J. Dellinger and C. Roberts, *J. Polym. Sci., Polym. Lett. Ed.*, 1976, **14**, 167–178.